Nickel and Palladium Complexes of Ferrocene-Backbone Bisphosphine-Borane and Trisphosphine Ligands

Bradley E. Cowie and David J. H. Emslie*

Department of Chemistry and Chemical Biology, McMaster University, 1280 Main Street West, Hamilton, Ontario, L8S 4M1, Canada.

Supporting Information Placeholder

ABSTRACT: Reaction of a ferrocene-backbone bisphosphine-borane ligand, [Fe(η^5-$C_5H_4PPh_2$)(η^5-$C_5H_4P^tBu$\{C_6H_4(BPh_2)-*o*\})] (FcPPB), with [Ni(cod)$_2$] (cod = 1,5-cyclooctadiene) or 0.5 equivalents of [Pd_2(dba)$_3$] (dba = *trans*,*trans*-dibenzylideneacetone) afforded [Ni(FcPPB)] (**1**) and [Pd(FcPPB)] (**2**), respectively; compound **1** does not react with dba. The FcPPB ligand in complexes **1** and **2** is coordinated via both phosphine donors as well as an η^3*BCC*-interaction with boron and the *ipso*- and *ortho*-carbon atoms of a *B*-phenyl group. The triphosphine analogue of the FcPPB ligand, [Fe(η^5-$C_5H_4PPh_2$)(η^5-$C_5H_4P^tBu$\{C_6H_4(PPh_2)-*o*\})] (FcPPP), was prepared by lithiation of [Fe(η^5-$C_5H_4PPh_2$)(η^5-$C_5H_4P^tBu$(C_6H_4Br-*o*)] followed by addition of Ph2PCl, and reaction of FcPPP with [Ni(cod)$_2$] provided "Ni(FcPPP)" (**3**), which exists as a mixture of isomers in which the FcPPP ligand is κ^3*PPP*-coordinated. Attempts to obtain X-ray quality crystals of **3** were derailed by its propensity to react with traces of N_2 within an argon-filled glovebox, yielding *rac*-[{Ni(FcPPP)\}$_2$(μ-N_2)] (**4**), in which two nickel(0) centers are linked by an end-on bridging N_2 unit. By contrast, reaction of FcPPP with 0.5 equivalents of [Pd_2(dba)$_3$] provided [Pd(η^2-dba)(FcPPP)] (**5**), in which the FcPPP ligand is κ^2*PP*-coordinated, and one equivalent of dba remains η^2*CC*-coordinated to palladium. Complexes **3** and **4** also reacted with dba, forming a new compound tentatively assigned as [Ni(η^2-dba)(FcPPP)] (**6**). Complexes **1**, **2** and **5** did not react with N_2.

INTRODUCTION

Ambiphilic ligands, defined as those containing one or more conventional Lewis basic donors accompanied by a σ-acceptor group (e.g. a group 13 Lewis acid), have enjoyed increasing popularity over the last 10 years.[1] Within this group, borane-containing ligands have played the dominant role, and are either generated *in situ*, typically from a hydroborate or related anionic ligand complex,[2-4] or are isolated prior to reaction with a metal precursor.[5-15] The most commonly employed borane-containing ligands are the $H_{3-x}B(mt)_x$ (mt = *N*-methylthioimidazolyl; x = 2 or 3) ligands pioneered by Hill,[2] and the $R_{3-x}B\{C_6H_4(PR_2)\text{-}o\}_x$ (x = 1-3) ligands developed by Bourissou.[5,6]

For ambiphilic ligand metal-borane complexes, η^1*B*-coordination, where the borane is a Z-type ligand (a zero-electron donor), is the most common binding mode.[1] However, η^2*BC*-,[9,16-21] η^3*BCC*-,[7,9,12,14,18,19,21-24] η^4*BC*$_3$-,[14,25] and even η^7*BC*$_6$-[18] and η^4*BCCP*-coordination[26] has been observed for arylborane- and/or vinylborane-containing ambiphilic ligands. Additionally, a variety of metal–(co-ligand)–borane interactions have been reported, where the co-ligand is an X-type ligand such as a halide[6,10,20,27] or a hydride,[15,17,19,24,28-31] an L-type ligand, including dba (*trans*,*trans*-dibenzylideneacetone),[8] or an isonitrile,[32] or an LX-type ligand such as H_2N=NH.[10] Moreover, co-ligand abstraction by a pendant borane has been reported for fluoride,[20] hydride[31,33,34] and alkyl[13,35] co-ligands, and several instances of hydrocarbyl[11,34-36] or halide[37] exchange between a transition metal and a pendant borane have been described, in addition to small molecule insertion into a metal–boron bond[30,38] and pendant borane facilitated reduction of CO ligands.[39]

The Peters group has explored the reactivity and redox chemistry of first row transition metal (Fe-Cu) $R_{3-x}B\{C_6H_4(PR_2)\text{-}o\}_x$ (x = 2 or 3) complexes, and has capitalized upon the ability of borane-containing ambiphilic ligands to stabilize transition metal complexes in a range of oxidation states by variation of the metal–boron bond length and accommodation of an array of metal coordination geometries.[16,19,23,26,40] However, direct comparisons between the coordination behaviour of borane-containing ambiphilic ligands and conventional ligand analogues (ligands in which the borane is replaced by a σ-donor) are scarce,[41] especially for tridentate or tetradentate ligands; *vide infra*.

In some cases, the structures of ambiphilic ligand complexes (those containing metal-borane interactions) and their conventional donor counterparts are analogous; for example, [(TPP)FeF] (TPP = P\{C_6H_4(PPh_2)-*o*\}$_3$)[42] and [Na(12-C-4)$_2$][(SiP^{iPr}_3)Fe(N_2)] (12-C-4 = 12-crown-4; SiP^{iPr}_3 = Si\{C_6H_4(P^iPr_2)-*o*\}$_3$)[43] adopt the same distorted trigonal bipyramidal coordination geometry as [(TBP)FeX] (TBP = B\{C_6H_4(P^iPr_2)-*o*\}$_3$; X = Br, NH_2 or OH) and [(TBP)Fe(N_2)].[26,29] By contrast, [(PP^{Ph}P)AuCl] (**A** in Figure 1; $PP^{Ph}P$ = PhP($C_6H_4PPh_2$-*o*)$_2$)[44] is pseudo-tetrahedral whereas [(^{Ph}DPB^{iPr})AuCl] (**B**; ^{X}DPB^R = X-B($C_6H_4PR_2$-*o*)$_2$)[45] approaches square planarity at gold. Additionally, while

[(SiP$^{iPr}_3$)Fe(CO)Na(THF)$_3$] (**C**)[46] is almost a perfect trigonal bipyramid at iron, [(TBP)Fe(CO)] (**D**)[26] features η^4*BCCP*-coordination, leading to a more complex geometry. Furthermore, while [{(PP^{Me}P)Ni}$_2$(μ-N$_2$)] (**E**; PP^{Me}P = MeP(C$_6$H$_4$PPh$_2$-*o*)$_2$),[47] [{(^{Ph}DPB^{iPr})Ni}$_2$(μ-N$_2$)] (**F**) and [(^{Ph}DPB^{Ph})Ni(THF)][29] are pseudo-tetrahedral, albeit with an η^2*BC*-arylborane interaction and more acute P–M–P angles in the ^{Ph}DPB^{R} complexes, related [(^{Mes}DPB^{Ph})Ni] (**G**; Mes = 2,4,6-trimethylphenyl) features an η^3*BCC*-arylborane interaction, and does not coordinate N$_2$ or THF (Figure 1).[29]

Herein we compare the coordination behaviour of a recently prepared ferrocene-backbone ambiphilic ligand, [Fe(η^5-C$_5$H$_4$PPh$_2$)(η^5-C$_5$H$_4$P^{t}Bu{C$_6$H$_4$(BPh$_2$)-*o*})] (FcPPB)[9] with that of the tris-phosphine analogue, [Fe(η^5-C$_5$H$_4$PPh$_2$)(η^5-C$_5$H$_4$P^{t}Bu{C$_6$H$_4$(PPh$_2$)-*o*})] (FcPPP) (Scheme 1), highlighting trends in the propensity of the resultant palladium and nickel complexes to bind dba and N$_2$.

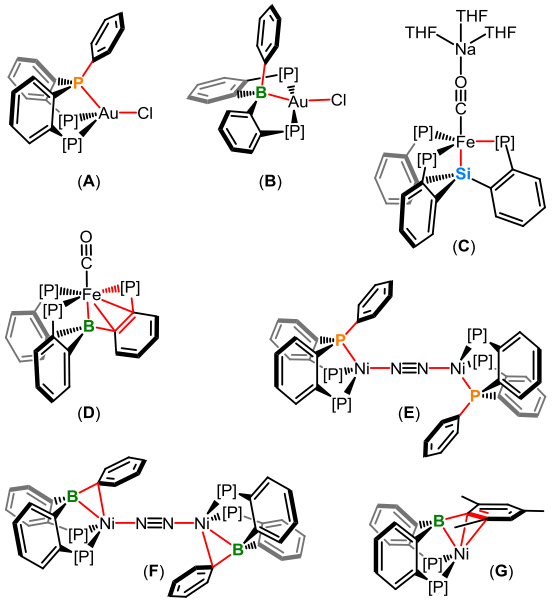

Figure 1. Tris-phosphine and tris-phosphine-silyl ligand complexes compared with analogues in which one neutral phosphine or anionic silyl donor is replaced with a borane Lewis acid. [P] = PPh$_2$ or P^{i}Pr$_2$ (see text).

RESULTS AND DISCUSSION

The FcPPB ligand was synthesized from [Fe(η^5-C$_5$H$_4$PPh$_2$){η^5-C$_5$H$_4$P^{t}Bu(C$_6$H$_4$Br-*o*)}] as previously reported (Scheme 1).[9] Reaction of FcPPB with either [Ni(cod)$_2$] (cod = 1,5-cyclooctadiene) or [Pd$_2$(dba)$_3$] (dba = *trans,trans*-dibenzylideneacetone) in toluene afforded [Ni(FcPPB)] (**1**) and [Pd(FcPPB)] (**2**), which were isolated as brick red and bright yellow solids in 78 and 63 % yield, respectively (Scheme 2). Both complexes feature low frequency solution ^{11}B NMR chemical shifts (28 and 23 ppm for **1** and **2**, respectively), indicative of metal–borane coordination.[48] Furthermore, both complexes feature *cis*-κ^2*PP*-coordination, as evidenced by ^{31}P{^{1}H} NMR chemical shifts of 47.3 and 12.2 ppm ($^2J_{P,P}$ 29 Hz in C$_6$D$_6$) for **1**, and 43.9 and 11.9 ppm ($^2J_{P,P}$ 19 Hz in CD$_2$Cl$_2$) for **2**; in both cases, ^{1}H-^{31}P HMBC NMR spectroscopy allowed assignment of the higher frequency ^{31}P signal to the C$_5$H$_4$*P*^{t}BuAr moiety.

Scheme 1. Synthesis of the FcPPB[9] and FcPPP ligands from [Fe(η^5-C$_5$H$_4$PPh$_2$){η^5-C$_5$H$_4$P^{t}Bu(C$_6$H$_4$Br-*o*)}].

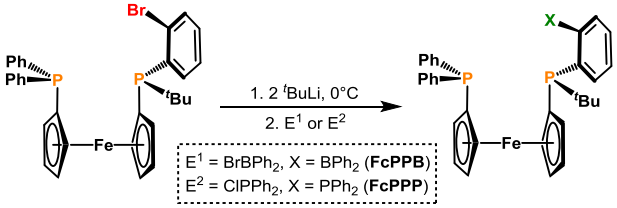

Scheme 2. Synthesis of [Ni(FcPPB)] (1) and [Pd(FcPPB)] (2).

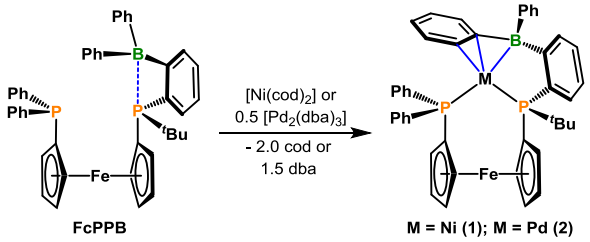

X-ray quality crystals of **1**·0.7(C$_7$H$_8$) and **2**·C$_2$H$_4$Cl$_2$ were obtained by slow diffusion of hexanes into a –30 °C solution of **1** in toluene or **2** in 1,2-dichloroethane. The solid-state structures of **1**·0.7(C$_7$H$_8$) and **2**·C$_2$H$_4$Cl$_2$ are shown in Figures 2 and 3, and in both cases the FcPPB ligand is coordinated to the metal center via both phosphine donors as well as an η^3*BCC*-interaction with boron and the *ipso*- and *ortho*-carbon atoms of a *B*-phenyl group; the M–B, M–C$_{ipso}$ and M–C$_{ortho}$ bond lengths are 2.220(4), 2.058(4) and 2.101(4) Å in **1**, and 2.279(4), 2.254(3) and 2.456(3) Å in **2**, and the P(1)–M–P(2) (M = Ni, Pd) bite angles in **1** and **2** are 107.71(4)° and 112.07(3)°, respectively. The metal center in **1** and **2** assumes a highly distorted square planar geometry, with '*trans*' P(1)–M–B and P(2)–M–C$_{ipso}$/C$_{ortho}$ angles of 151.3(1) and 132.7(1)° in **1**, and 163.8(1) and 128.1(1)° in **2** (M = Ni and Pd; C$_{ipso}$/C$_{ortho}$ = centroid between C$_{ipso}$ and C$_{ortho}$). In complex **1**, P(1), P(2), Ni, C$_{ipso}$ and C$_{ortho}$ form a plane, with B(1) located 1.072 Å out of the plane. By contrast, in complex **2**, P(1), P(2), Pd, B(1) and C$_{ortho}$ lie approximately in the same plane, with C$_{ipso}$ located 0.763 Å from the plane. In compound **1**, the non-coordinated *B*-phenyl ring is oriented away from the *tert*-butyl group on the central phosphine, whereas in **2**, it is positioned above the *tert*-butyl group.

Boron is planar in **1** and only slightly pyramidalized in **2**, with the sum of the C–B–C angles equal to 359.1(6) and 354.8(5)°, respectively. A similar η^3*BCC*-interaction was previously observed in [Pt(FcPPB)], with Σ(CBC) equal to 354.3(5)° and an ^{11}B NMR chemical shift of 20 ppm,[9] suggestive of a slightly stronger metal–boron interaction in the platinum complex. However, despite observation of η^3*BCC*-coordination in the solid-state structures of **1** and **2** (and the platinum analogue), the *ortho*- and *meta* protons on the *B*-phenyl rings remain equivalent in the ^{1}H NMR spectra of these complexes from 25 to –90 °C, indicating that the η^3*BCC*-interaction is not maintained in solution.

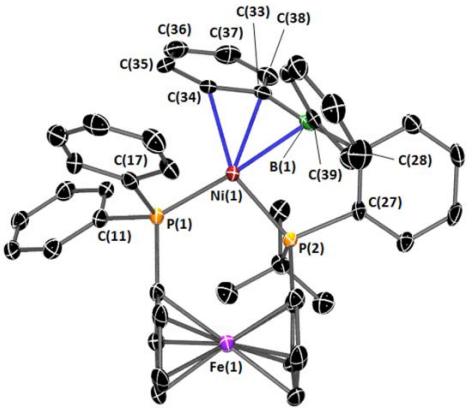

Figure 2. Solid-state structure of **1**·0.7(C_7H_8) with ellipsoids drawn at 50% probability. Hydrogen atoms and solvent are omitted for clarity. Selected bond lengths [Å] and angles [°]: Ni(1)–P(1), 2.189(1); Ni(1)–P(2), 2.153(1); Ni(1)–B(1), 2.220(4); Ni(1)–C(33), 2.058(4); Ni(1)–C(34), 2.101(4); B(1)–C(33), 1.526(6); B(1)–C(28), 1.607(6); B(1)–C(39), 1.614(6); C(33)–C(34), 1.443(5); P(1)–Ni(1)–P(2), 107.71(4); P(1)–Ni(1)–C(34), 99.5(1); P(1)–Ni(1)–C(33), 140.1(1); P(2)–Ni(1)–B(1), 82.9(1); P(2)–Ni(1)–C(34), 152.7(1); P(2)–Ni(1)–C(33), 112.1(1); P(1)–Ni(1)–B(1), 151.3(1); C(28)–B(1)–C(33), 125.4(4); C(28)–B(1)–C(39), 111.0(3); C(33)–B(1)–C(39), 122.7(4).

The B–C_{ipso} bond length in **1** is 1.526(6) Å, which is significantly contracted relative to the other two B–C_{aryl} bonds (B–C(28) = 1.607(6) Å, B–C(39) = 1.614(6) Å). The B–C_{ipso} bonds in **2** and [Pt(FcPPB)] are also somewhat contracted, with B–C_{ipso} distances of 1.563(6) and 1.551(5) Å, respectively (the remaining B–C_{aryl} distances lie between 1.596(6) and 1.611(4) Å).[9] For comparison, the B–C_{α} bond distances in the vinylborane and borataalkene complexes [Ni(PPh_3)$_2$(VB^{Ph})] (VB^{Ph} = (*E*)-PhHC=CH–B(C_6F_5)$_2$), [Pd(P^tBu_3)(VB^{Ph})],[49] [Cp_2Ta(CO){η^2*BC*-H_2CB(C_6F_5)$_2$}][50] and [Cp_2Ta(CN^tBu)-{η^2*BC*-H_2CB(C_6F_5)$_2$}][51] are 1.483(4), 1.517(6)/1.519(7), 1.508(8) and 1.525(7) Å, respectively. The coordinated *B*-phenyl ring in **1** also shows considerable bond alternation with C(33)–C(34), C(34)–C(35), C(35)–C(36), C(36)–C(37), C(37)–C(38) and C(33)–C(38)) distances of 1.443(5), 1.423(6), 1.365(7), 1.412(7), 1.354(6) and 1.449(6) Å, respectively. Similar bond alternation is also observed in **2** and [Pt(FcPPB)], with the equivalent bond lengths equal to 1.424(5), 1.404(6), 1.371(7), 1.397(6), 1.376(5) and 1.427(5) Å in **2**, and 1.443(4), 1.423(5), 1.360(5), 1.418(4), 1.368(5) and 1.437(4) Å in [Pt(FcPPB)]. Furthermore, comparable bond length alternations have been observed by Peters and co-workers in η^n*BC*$_{n-1}$- (n = 3 or 4) coordinated arylborane complexes.[18,19,26]

The Ni–B bond length in **1** is significantly contracted relative to the Ni–B bond length in previously reported [Ni(TXPB)] (TXPB (Scheme 3) = 2,7-di-tert-butyl-5-diphenylboryl-4-diphenylphosphino-9,9-dimethylthio-xanthene;) [2.297(4) Å], while the Ni–C_{ipso} and Ni–C_{ortho} bond lengths in **1** are significantly elongated relative to those found in [Ni(TXPB)] [Ni–C_{ipso} = 2.019(3) Å; Ni–C_{ortho} = 2.081(3) Å].[22] The same trend is observed in the comparison of **2** with previously reported [Pd(TXPB)] [Pd–B = 2.320(5) Å; Pd–C_{ipso} = 2.198(4) Å; Pd–C_{ortho} = 2.325(4) Å].[22] This trend may reflect (a) differences in the backbone of the ligands, which alter the distance and orientation of the BCC unit relative to the metal coordination pocket defined by the phosphine donors, and/or (b) an intrinsically stronger metal–borane interaction in the FcPPB complexes due to the improved donor ability of the central phosphine in FcPPB, relative to the diarylthioether moiety in TXPB. For comparison, the [Ni(^{Ph}DPB^{Mes})] [^{Ph}DPB^{Mes} = {*o*-(Ph_2P)C_6H_4}$_2$BMes] complex reported by Peters also features η^3*BCC*-coordination of the arylborane, and in this case the Ni–B distance (2.1543(9) Å) is shorter than that in **1**, while the Ni–C_{ipso} and Ni–C_{ortho} bond lengths (2.0751(8) and 2.1616(8) Å, respectively) are longer than those in **1**.[19]

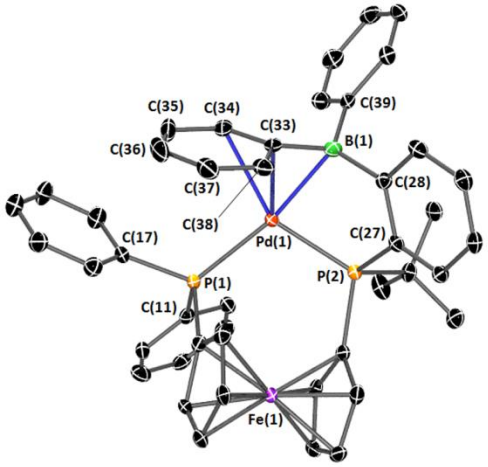

Figure 3. Solid-state structure of **2**·$C_2H_4Cl_2$ with ellipsoids drawn at 50% probability. Hydrogen atoms and solvent have been omitted for clarity. Selected bond lengths [Å] and angles [°]: Pd(1)–P(1), 2.3530(9); Pd(1)–P(2), 2.282(1); Pd(1)–B(1), 2.279(4); Pd(1)–C(33), 2.254(3); Pd(1)–C(34), 2.456(3); B(1)–C(33), 1.563(6); B(1)–C(28), 1.597(5); B(1)–C(39), 1.596(6); C(33)–C(34), 1.424(5); P(1)–Pd(1)–P(2), 112.07(3); P(1)–Pd(1)–C(34), 100.15(9); P(1)–Pd(1)–C(33), 123.6(1); P(1)–Pd(1)–B(1), 163.8(1); P(2)–Pd(1)–B(1), 78.9(1); P(2)–Pd(1)–C(33), 110.3(1); P(2)–Pd(1)–C(34), 144.22(9); C(28)–B(1)–C(33), 116.2(3); C(28)–B(1)–C(39), 119.8(3); C(33)–B(1)–C(39), 118.8(3).

Surprisingly, the reaction of FcPPB with [Pd_2(dba)$_3$] differs from the reaction of TXPB with [Pd_2(dba)$_3$]; the latter reaction affords [Pd(μ-dba)(TXPB)], in which dba is η^3*CCC*-coordinated to palladium and κ^1*O*-coordinated to boron, yielding a zwitterionic palladium(II) boratoxyallyl (CHPhCHCR–O–BAr_3) complex (Scheme 3).[8] The divergent reactivity of FcPPB and TXPB can most straightforwardly be rationalized on the basis of steric differences in the ambiphilic ligand backbones, given that greater electron donation from the central donor of FcPPB versus TXPB would be expected to promote zwitterion formation.

In order to probe the extent to which the coordination chemistry of the FcPPB ligand differs from that of a conventional tridentate ligand, a trisphosphine analogue of FcPPB, [Fe(η^5-$C_5H_4PPh_2$)(η^5-$C_5H_4P^tBu${C_6H_4(PPh_2)-*o*})] (FcPPP) was developed. This FcPPP ligand was synthesized following a route analogous to that used to prepare FcPPB, but with the addition of Ph_2PCl, rather than Ph_2BBr, to [Fe(η^5-$C_5H_4PPh_2$)(η^5-$C_5H_4P^tBu$(C_6H_4Li-*o*)] (Scheme 1).

Scheme 3. Reaction of TXPB with $Pd_2(dba)_3$.[8]

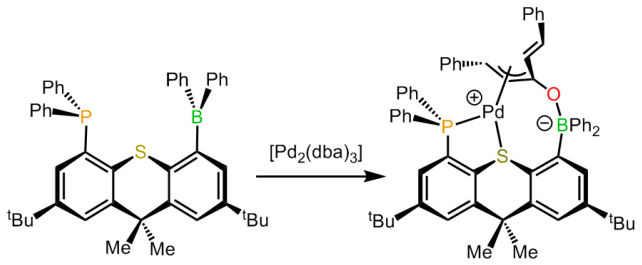

Reaction of FcPPP with $[Ni(cod)_2]$ yielded a red/orange solid in 87 % yield (Scheme 4). While elemental analysis (C and H) indicates the stoichiometry of the product is "Ni(FcPPP)" (**3**), ^{1}H and ^{31}P{^{1}H} NMR spectra between 195 and 348 K feature numerous broadened signals (15 signals in the ^{31}P NMR spectrum at 195 K), consistent with a mixture of isomers in rapid equilibrium. Importantly though, all signals in the ^{31}P{^{1}H} NMR spectra are located between 60 and 15 ppm, indicative of κ^3*PPP*-coordination, which suggests the involvement of multinuclear complexes, rather than complexes featuring different FcPPP ligand denticities.

Scheme 4. Synthesis of "Ni(FcPPP)" (3), and subsequent reaction with N_2 to afford *rac*-[{Ni(FcPPP)}$_2$(μ-N_2)] (4).

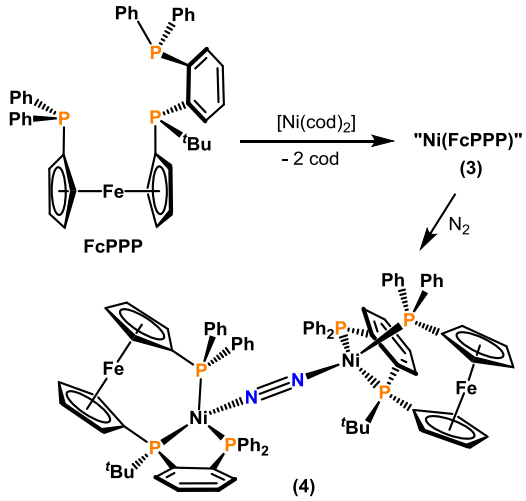

Attempts were made to obtain X-ray quality crystals of **3** by slow diffusion of hexanes into a solution of **3** in benzene at room temperature in an argon-filled glove box. However, ruby red crystals of *rac*-[{Ni(FcPPP)}$_2$(μ-N_2)]·(C_6H_6)(C_6H_{14}) [**4**·(C_6H_6)(C_6H_{14})] (Figure 4) were invariably isolated due to the reaction of **3** with trace nitrogen in the glovebox atmosphere. Dimetallic **4** was also isolated on a preparative scale in 64 % yield by placing a solution of **3** in benzene/hexanes under 1 atm. of N_2 at room temperature (Scheme 4). Complex **4** is stable *in vacuo* in the solid-state, and is only slightly soluble in THF; N_2 is not displaced by THF after days in solution. In THF-d_8, compound **4** gives rise to signals at 51.6, 35.6 and 19.2 ppm in the ^{31}P{^{1}H} NMR spectrum ($^2J_{P,P}$ = 59-87 Hz), which are in the same range as the signals observed for **3**. Clean conversion of **3** to **4** further supports the identification of **3** as "Ni(FcPPP)".

In the solid state structure of **4**, a molecule of N_2 bridges between two Ni(FcPPP) units. The Ni–P(1), Ni–P(2) and Ni–P(3) bond lengths are 2.1699(5), 2.1643(5) and 2.1474(5) Å, respectively, and the geometry of each nickel center is pseudo-tetrahedral, with the P–Ni–P and P–Ni–N angles ranging from 91.50(2) to 118.32(5)°. The bridging N_2 unit is coordinated end-on [Ni–N(1)–N(1') = 174.12(7)°] to both Ni centers with a Ni–N bond distance of 1.840(2) Å, and a N≡N distance of 1.122(3) Å, which is only very slightly elongated relative to that in free N_2.

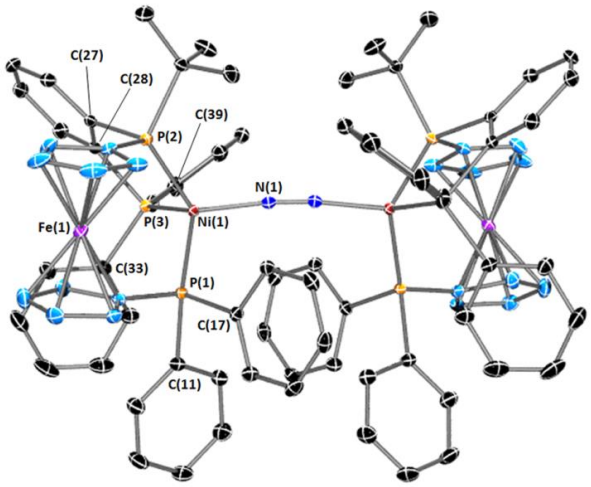

Figure 4. Solid-state structure of **4**·(C_6H_6)(C_6H_{14}) with ellipsoids drawn at 50% probability. Hydrogen atoms and solvent have been omitted, and cyclopentadienyl carbon atoms are coloured light blue for clarity. Selected bond lengths [Å] and angles [°]: Ni(1)–P(1), 2.1699(5); Ni(1)–P(2), 2.1643(5); Ni(1)–P(3), 2.1474(5); Ni(1)–N(1), 1.840(2); N(1)–N(1'), 1.122(3); P(1)–Ni(1)–P(2), 110.48(2); P(1)–Ni(1)–P(3), 113.39(2); P(2)–Ni(1)–P(3), 91.50(2); P(1)–Ni(1)–N(1), 105.61(5); P(2)–Ni(1)–N(1), 118.32(5); P(3)–Ni(1)–N(1), 117.39(5); Ni(1)–N(1)–N(1'), 174.12(7).

Very similar structural features were observed in [{Ni(PP^{R}P)}$_2$(μ-N_2)] (PP^{R}P = {*o*-(^{i}Pr$_2$P)C_6H_4}$_2$PR; R = Me, OMe) reported by Lee and co-workers, in which each Ni center is also pseudo-tetrahedral with Ni–N bond lengths of 1.830(2) and 1.837(4) Å, N–N bond lengths of 1.124(3) and 1.112(5) Å, and Ni–N–N bond angles of 178.6(2) and 176.3(4)°, respectively (in solution under N_2, both dimetallic complexes exist in equilibrium with a monometallic N_2-species).[52,53] Peters *et al.* have also reported the synthesis of [Ni(N_2)(^{iPr}DPB^{Ph})] (^{iPr}DPB^{Ph} = {*o*-(^{i}Pr$_2$P)C_6H_4}$_2$BPh), which crystallized with three independent molecules within the unit cell, two of which are [Ni(N_2)(^{iPr}DPB^{Ph})] and one of which is [{Ni(^{iPr}DPB^{Ph})}$_2$(μ-N_2)]. Similarly to **4**, the nickel center in the dimetallic compound is pseudo-tetrahedral with Ni–N and N–N bond lengths of 1.920(1) and 1.123(3) Å, respectively.[17] The N≡N stretching frequency in **4** is 2006 cm^{-1}, which is shifted to lower frequency relative to the aforementioned [{Ni(PP^{R}P)}$_2$(μ-N_2)] complexes (ν(N≡N) = 2045 cm^{-1} (R = Me) and 2038 cm^{-1} (R = OMe)). However, it is consistent with the crystallographically determined N–N bond length, according to the plot of N–N bond distance versus N–N stretching frequency in a 2010 review by Holland.[52]

Scheme 5. Synthesis of [Pd(η²-dba)(FcPPP)] (5) from FcPPP and [Pd₂(dba)₃].

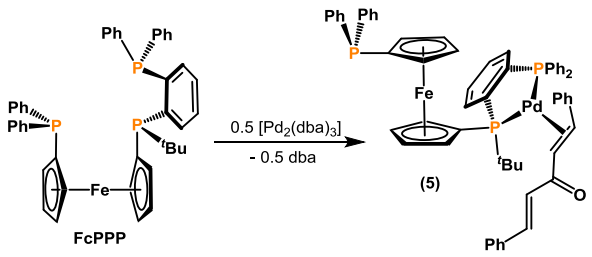

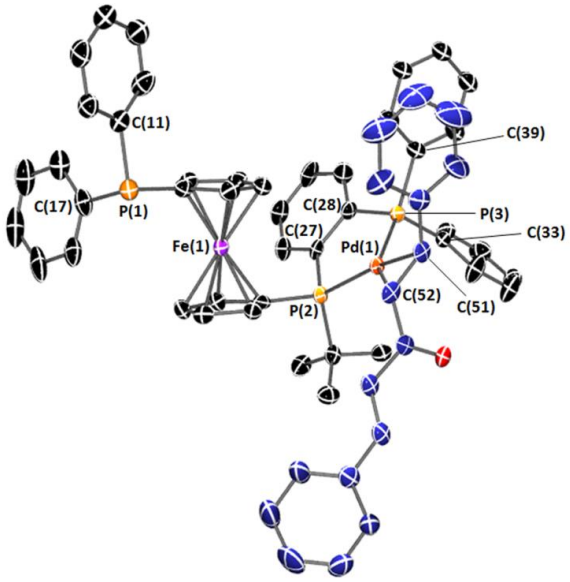

Figure 5. Solid-state structure of **5**·CH_2Cl_2 with ellipsoids drawn at 50% probability. Hydrogen atoms and solvent are omitted, and the carbon atoms of the η^2*CC*-coordinated dba co-ligand are coloured navy blue for clarity. The *P*-phenyl ring containing atoms C39–C44 is disordered over two positions; position B is omitted for clarity. Selected bond lengths [Å] and angles [°]: Pd(1)–P(1), 7.500(2); Pd(1)–P(2), 2.308(2); Pd(1)–P(3), 2.253(2); Pd(1)–C(51), 2.113(6); Pd(1)–C(52), 2.160(6); C(51)–C(52), 1.416(9); C(54)–C(55), 1.315(9) Å; P(2)–Pd(1)–P(3), 87.11(6); P(2)–Pd(1)–C(51), 164.8(2); P(2)–Pd(1)–C(52), 126.2(2); P(3)–Pd(1)–C(51), 108.0(2); P(3)–Pd(1)–C(52), 146.7(2); C(51)–Pd(1)–C(52), 38.7(2).

The reaction of FcPPP with 0.5 equivalents of $[Pd_2(dba)_3]$ produced a bright orange solid in 76 % yield, identified as [Pd(η^2-dba)(FcPPP)] (**5**) (Scheme 5). Elemental analysis is consistent with this formulation, but similarly to **3**, complete characterization of **5** by ^{1}H and ^{13}C NMR spectroscopy was hampered by fluxional behaviour involving multiple solution isomers. Nevertheless, the room temperature $^{31}P\{^1H\}$ NMR spectrum of **5** gave rise to broad singlets at 57.3, 38.9 and –16.7 ppm ($\omega_{1/2}$ 150 Hz, C_6D_6), indicative of an equilibrium between κ^2*PP*- rather than κ^3*PPP*-coordinated isomers. These signals decoalesce at low temperature, and at 230 K, the non-coordinated $C_5H_4PPh_2$ phosphine signal split into four sharp singlets at –17.90, –18.16, –18.22 and –18.25 ppm in an approximate 6:2:3:3 ratio, consistent with four κ^2*PP*-coordinated solution isomers. Furthermore, four *tert*-butyl resonances were observed in the ^{1}H NMR spectrum of **5** at 230 K, with $^3J_{H,P}$ couplings of 12-15 Hz.

X-ray quality crystals of **5**·CH_2Cl_2 were obtained by slow diffusion of hexanes into a solution of **5** in CH_2Cl_2 at –30 °C (Figure 5). The solid-state structure of **5**, representing one of the accessible solution isomers, confirms κ^2*PP*-coordination via the $C_5H_4P^t$BuAr and Ar*P*Ph_2 phosphines, with an acute P(2)–Pd–P(3) bite angle of 87.11(6)°, and Pd–P(2) and Pd–P(3) bond lengths of 2.308(2) and 2.253(2) Å; the $C_5H_4PPh_2$ phosphine remains uncoordinated and is positioned 7.500(2) Å from the metal center. One molecule of dba is η^2*CC*-coordinated to palladium, with Pd–C(51) and Pd–C(52) bond lengths of 2.113(6) and 2.160(6) Å. The C–C bond length of the η^2*CC*-coordinated unit [C(51)–C(52)] is 1.416(9) Å, which is significantly elongated relative to the C=C bond of free dba (1.315(9) Å). Similar deviations in C–C bond lengths are observed in [Pd(η^2-dba)(PPh_3)$_2$], [Pd(η^2-dba)(PCy_3)$_2$][54] and [Pd(η^2-dba){κ^2*PP*-{*o*-(^{i}Pr_2P)C_6H_4}$_2$$CH_2$}],[55] consistent with a metallacyclopropane bonding mode for the coordinated alkene. The geometry at palladium in **5** is pseudo-square planar, with P(2)–Pd–C(51) and P(3)–Pd–C(52) bond angles equal to 164.8(2) and 146.7(2)°.

The inability of FcPPP ligand to completely displace dba from palladium contrasts the reactivity of FcPPB with $[Pd_2(dba)_3]$. Similarly, [Ni(TXPB)] (**1**) did not react with dba, whereas FcPPP complexes **3** and **4** reacted with dba to form a new product, presumably [Ni(η^2-dba)(FcPPP)] (**6**); this compound exists as two major isomers in solution at room temperature, as evidenced by two distinct *tert*-butyl resonances in the ^{1}H NMR spectrum at 0.95 and 0.71 ppm ($^3J_{H,P}$ 14 Hz).

CONCLUSIONS

The observation that FcPPB reacts with $[Pd_2(dba)_3]$ to generate dba-free [Pd(FcPPB)] (**2**) while FcPPP forms [Pd(η^2-dba)(FcPPP)] (**5**) leads to the unanticipated conclusion that in the present work, FcPPB is a superior ligand relative to FcPPP; effectively, after coordination of two phosphine donors in FcPPB or FcPPP to palladium, the binding preference for follows the order BAr_3 > dba > PR_3 (where BAr_3 and PR_3 are pendant borane and phosphine groups of the FcPPB and FcPPP ligands, respectively). The same binding preference is observed for nickel, since [Ni(TXPB)] (**1**) does not react with dba, whereas "Ni(FcPPP)" (**3**) and *rac*-[{Ni(FcPPP)}$_2$(μ-N_2)] (**4**) react with dba to form a new product tentatively assigned as [Ni(η^2-dba)(FcPPP)] (**6**). Additionally, while "Ni(FcPPP)" (**3**) reacts readily with even traces of N_2, FcPPB compounds **1** and **2** do not react with N_2. Compound **5** also did not react with N_2 due to preferential dba coordination. The much greater tendency of arylboranes versus arylphosphines to engage in polyhapto coordination can be attributed to the potential for delocalization within the η^n-coordinated BC_{n-1} fragment ($n \geq 2$),[7] and the approximate trigonal planarity of boron in η^n*BC*$_{n-1}$-coordinated complexes, which allows for close approach of the aryl substituents on boron to the metal.

EXPERIMENTAL SECTION

An argon-filled MBraun UNIlab glove box equipped with a −30 °C freezer was employed for the manipulation and storage of the FcPPB

and FcPPP ligands along with their complexes, and reactions were performed on a double manifold high vacuum line using standard techniques.[56] A Fisher Scientific Ultrasonic FS-30 bath was used to sonicate reaction mixtures where indicated. A VWR Clinical 200 Large Capacity Centrifuge (with 28° fixed-angle rotors that hold 12 × 15 mL or 6 × 50 mL tubes) in combination with VWR high-performance polypropylene conical centrifuge tubes was used when required (inside the glovebox). Residual oxygen and moisture was removed from the argon stream by passage through an Oxisorb-W scrubber from Matheson Gas Products.

Toluene and hexamethyldisiloxane [$O(SiMe_3)_2$] were dried and distilled at atmospheric pressure from Na. Benzene and hexanes were initially dried and distilled at atmospheric pressure from Na/Ph_2CO. Unless otherwise noted, all proteo solvents were stored over an appropriate drying agent (toluene, benzene = Na/Ph_2CO; hexanes, $O(SiMe_3)_2$ = Na/Ph_2CO/tetra-glyme) and introduced to reactions via vacuum transfer with condensation at −78 °C. Deuterated solvents (ACP Chemicals) were dried over Na/Ph_2CO (C_6D_6, THF-d_8, Toluene-d_8) or CaH_2 (CD_2Cl_2).

^{t}BuLi solution (1.7 M in pentane), *trans*,*trans*-dibenzylideneacetone, [$Pd_2(dba)_3$] and Cl–PPh_2 were purchased from Sigma-Aldrich and stored under argon. ^{t}BuLi was isolated as a solid by evaporation of the pentane *in vacuo*, and Cl–PPh_2 was dried over molecular sieves (4 Å) and distilled *in vacuo* prior to use. [$Ni(cod)_2$] was purchased from Strem Chemicals and stored under argon. Argon and N_2 of 99.999 % purity were purchased from Praxair. [Fe(η^5-$C_5H_4PPh_2$){η^5-$C_5H_4P(^tBu)(C_6H_4Br$-*o*)}] and FcPPB[9] were prepared according to the literature procedures.

Raman spectra were collected on a Renishaw Invia Laser Raman microscope equipped with 785 nm excitation. For complex **4**, the 1200 lines per mm grating and 5× objective was employed, with the laser set to 50% power and the spectrum collected from 100 to 3200 cm^{-1}. Combustion elemental analyses were performed on a Thermo EA1112 CHNS/O analyzer. NMR spectroscopy (^{1}H, ^{13}C{^{1}H}, ^{31}P{^{1}H}, ^{11}B, ^{13}C-DEPT-135, ^{13}C-uDEFT, ^{1}H-^{1}H-COSY, ^{1}H-^{13}C-HSQC, ^{1}H-^{13}C-HMBC, ^{1}H-^{31}P-HMBC) was performed on Bruker DRX-500 and AV-600 spectrometers. All ^{1}H NMR and ^{13}C{^{1}H} NMR spectra were referenced relative to $SiMe_4$ through a resonance of the employed deuterated solvent or proteo impurity of the solvent; C_6D_6 (7.16 ppm), THF-d_8 (3.58, 1.72) and CD_2Cl_2 (5.32 ppm) for ^{1}H NMR; C_6D_6 (128.0 ppm), THF-d_8 (67.21, 25.31 ppm) and CD_2Cl_2 (54.00 ppm) for ^{13}C NMR. ^{31}P{^{1}H} and ^{11}B NMR spectra were referenced using an external standard of 85% H_3PO_4 in D_2O (0.0 ppm) and $BF_3{\cdot}OEt_2$ (0.0 ppm), respectively. Temperature calibration was performed using a d_4-methanol sample, as outlined in the Bruker VTU user manual.

Herein, numbered proton and carbon atoms refer to the positions of the C_5H_4 rings and the phenylene linker within the FcPPB and FcPPP ligand backbones. The C_5H_4 ring bound to the $C_5H_4P(^tBu)$Ar phosphine was numbered $C^{1'\text{-}5'}$, where $C^{1'}$ is the *ipso*-carbon atom bound to phosphorus, and the C_5H_4 ring bound to the $C_5H_4PPh_2$ phosphine was numbered $C^{1''\text{-}5''}$, where $C^{1''}$ is the *ipso*-carbon atom bound to phosphorus. Following installation of either the –BPh_2 or –PPh_2 groups in FcPPB and FcPPP, respectively, the phenylene linker of the ligand backbone was numbered such that C^1 refers to the carbon atom bound to the *tert*-butylphosphine moiety, and C^2 refers to the carbon atom bound to the diphenylborane or diphenylphosphine, respectively. The remainder of the carbon atoms and protons in the phenylene linker were numbered accordingly in both cases. Within the FcPPP ligand and its complexes, two different –PPh_2 groups are present. The –PPh_2 group bound to the C_5H_4 ring is referred to as PPh_2^{Cp}, and the –PPh_2 group bound to the phenylene linker is referred to as PPh_2^{Ar}; ^{1}H and ^{13}C resonances that correspond to the phenyl groups bound to each phosphine are labelled accordingly. Inequivalent phenyl rings on boron and phosphorus are labelled A and B so that the proton and carbon resonances belonging to a single phenyl ring can be identified. We did not identify which *B*-phenyl or *P*-phenyl rings give rise to the signals labelled A or B, respectively. The room temperature and variable temperature (195–348 K) ^{1}H NMR spectra for complexes **3** and **5** were either extremely broad or extremely complex due to the presence of multiple isomers in solution. As a result, unambiguous ^{1}H and ^{13}C NMR assignment was not typically possible for **3** and **5**, and only ^{31}P NMR chemical shifts are provided, as well as low temperature CMe_3 ^{1}H NMR chemical shifts for **5**.

X-ray crystallographic analyses were performed on suitable crystals coated in Paratone oil and mounted on a SMART APEX II diffractometer with a 3 kW Sealed tube Mo generator in the McMaster Analytical X-Ray (MAX) Diffraction Facility. In all cases, non-hydrogen atoms were refined anisotropically and hydrogen atoms were generated in ideal positions and then updated with each cycle of refinement. The $0.7(C_7H_8)$ solvent molecule in **1**$\cdot 0.7(C_7H_8)$ was SQUEEZED from the lattice through the use of the SQUEEZE routine due to unresolvable disorder.[57] The molecule of CH_2Cl_2 in **5**$\cdot CH_2Cl_2$ was positionally disordered over two positions in a 58:42 ratio. The carbon and chlorine atoms modeled as molecule A and B over the two positions (C62A, C62B, CL1A, CL1B, CL2A, CL2B) were restrained to have similar thermal parameters, respectively, through the use of the SIMU command. In addition, the carbon–chlorine bond distances in molecule B of the disordered CH_2Cl_2 molecule were fixed to ~1.77 Å through the use of the DFIX command. Finally, the spatial orientation of molecule B of the disordered CH_2Cl_2 molecule was modeled to be equivalent to that of molecule A through the use of the SAME command. One phenyl group (C39–C44) of **5**$\cdot CH_2Cl_2$ was also positionally disordered over two positions, however in a 51:49 ratio. The carbon atoms modeled as molecule A and B (C39A–C44B) were restrained to have similar thermal parameters through the use of the SIMU command. In addition, phenyl group A was restrained through the use of the AFIX 66 command. P(3) was also included in the refinement of phenyl ring C39–C44, and thus was split into P(3A) and P(3B), with the thermal and positional parameters being held equivalent through the use of the EADP and EXYZ commands, respectively.

[Ni(FcPPB)] (1): Toluene (25 mL) was condensed into a 50 mL round bottom flask containing [$Ni(cod)_2$] (114 mg, 0.413 mmol) and FcPPB (288 mg, 0.413 mmol) through the use of a dry ice/acetone bath. The reaction was left to stir for 4 hours at room temperature, over which time the initially orange solution progressively became blood red. The reaction mixture was then evaporated to dryness *in vacuo* leaving a dark red, oily residue. Hexanes (25 mL) were added to the crude residue and the resulting mixture was sonicated for 15 minutes, allowing for [Ni(FcPPB)] to precipitate from solution as a brick red powder. The hexanes solution was filtered and the collected product was washed with hexanes (2 × 10 mL) then dried *in vacuo*. Yield = 245 mg (78 %). X-ray quality crystals were obtained by slow diffusion of hexanes (~10 mL) into a solution of **2** (~25 mg) in toluene (~5 mL) at –30 °C. ^{1}H NMR (C_6D_6, 600 MHz, 298 K): δ 7.83 (app. q, $^3J_{H,H}$ 9 Hz, 3H, CH^6, *o*-PPh_2 A), 7.33 (t, $^3J_{H,H}$ 7 Hz, 1H, CH^5), 7.26–7.25 (m, 2H, *o*-BPh_2 A), 7.21 (t, $^3J_{H,H}$ 8 Hz, 2H, *o*-PPh_2 B), 7.17–7.13 (m, 3H, CH^3, *m*-BPh_2 A), 7.10–7.05 (m, 5H, CH^4, *p*-BPh_2 A, *m*,*p*-PPh_2 A), 6.94–6.90 (m, 6H, *m*,*p*-BPh_2 B, *m*,*p*-PPh_2 B), 6.81 (t, $^3J_{H,H}$ 7 Hz, 2H, *o*-BPh_2 B), 4.67 (s, 1H, C$H^{2'/5'}$), 4.27 (s, 1H, C$H^{5'/2'}$), 4.24 (s, 1H, C$H^{2''/5''}$), 4.13 (s, 1H, C$H^{5''/2''}$), 3.96 (s, 1H, C$H^{3'/4'}$), 3.93 (s, 1H, C$H^{4''/3''}$), 3.85 (s, 2H, C$H^{4'/3'}$, C$H^{3''/4''}$), 1.09 (d, $^3J_{H,P}$ 13 Hz, 9H, CMe_3). ^{13}C{^{1}H} NMR (C_6D_6, 151 MHz, 298 K): δ 162.8 (broad s, C^2), 143.5 (dd, $^1J_{C,P}$ 39, $^3J_{C,P}$ 11 Hz, C^1), 138.4 (dd, $^1J_{C,P}$ 28 Hz, $^3J_{C,P}$ 3 Hz, *ipso*-PPh_2 B), 136.6 (d, $^2J_{C,P}$ 17 Hz, *o*-PPh_2 A), 135.1 (d, $^1J_{C,P}$ 31 Hz, *ipso*-PPh_2 A), 133.1 (s, C^3), 132.6 (d, $^2J_{C,P}$ 26 Hz, C^6), 131.4 (d, $^2J_{C,P}$ 12 Hz, *o*-PPh_2 B), 130.5 (s, *p*-PPh_2 A), 129.8 (s, C^5), 129.2 (s, *o*-BPh_2 B), 128.5 (d, $^3J_{C,P}$ 9 Hz, *m*-PPh_2 A), 128.4 (d, $^3J_{C,P}$ 9 Hz, *m*-PPh_2 B), 128.4 (s, *m*-BPh_2 A), 128.3 (s, *p*-PPh_2 B), 125.8 (d, $^4J_{C,P}$ 6 Hz, C^4), 125.4 (s, *p*-BPh_2 B), 124.4 (s, *p*-BPh_2 A), 123.3 (s, *m*-BPh_2 B), 121.8 (s, *o*-BPh_2 A), 83.5 (d, $^1J_{C,P}$ 40 Hz, $C^{1''}$), 82.6 (d, $^1J_{C,P}$ 30 Hz, $C^{1'}$), 75.2 (d, $^2J_{C,P}$ 14 Hz, $C^{2'/5'}$), 74.2 (d, $^2J_{C,P}$ 12 Hz, $C^{2''/5''}$), 73.1 (d, $^3J_{C,P}$ 5 Hz, $C^{5''/2''}$), 72.6 (s, $C^{5'/2'}$), 71.1 (d, $^2J_{C,P}$ 7 Hz, $C^{3'/4'}$), 69.6 (d, $^3J_{C,P}$ 6 Hz, $C^{4''/3''}$), 69.4 (d, $^2J_{C,P}$ 3Hz, $C^{4'/3'}$), 69.1 (s, $C^{3''/4''}$), 35.1 (d, $^2J_{C,P}$ 21 Hz, CMe_3), 30.2 (d, $^2J_{C,P}$ 6 Hz, CMe_3); *ipso*-BPh_2 A could not be located. ^{31}P{^{1}H} (C_6D_6, 203 MHz, 298 K): δ 43.7 (d, $^2J_{P,P}$ 29 Hz, $C_5H_4P(^tBu)$Ar), 12.2 (d, $^2J_{P,P}$ 29 Hz, $C_5H_4PPh_2$). ^{11}B NMR (C_6D_6, 161 MHz, 298 K): δ 28 (broad s, $\omega_{1/2}$ = 2400 Hz). Anal. Calcd. For $C_{44}H_{41}BFeNiP_2$: C, 69.80 H, 5.46%. Found: C, 69.64; H, 5.75%.

[Pd(FcPPB)]·0.5CH_2Cl_2 (2): Toluene (30 mL) was condensed into a 50 mL round bottom flask containing [$Pd_2(dba)_3$] (215 mg, 0.235 mmol) and FcPPB (327 mg, 0.469 mmol) through the use of a dry ice/acetone bath, and the reaction was left to stir overnight at room temperature. The black/yellow reaction solution was filtered to remove any unreacted [$Pd_2(dba)_3$], and the residual solid was washed with 2 × 10 mL of toluene. The resulting clear, bright orange filtrate was evaporated to dryness *in vacuo*, leaving an orange, oily residue. Hexanes (25 mL) was added to the crude residue and the resulting mixture was sonicated for 15 minutes, allowing for [Pd(FcPPB)] to precipitate from solution as a yellow powder. The hexanes solution was filtered and the collected product was washed with hexanes (3 × 10 mL) then dried *in vacuo*. Yield = 237 mg (63 %). X-ray quality crystals, which were also utilized for elemental analysis, were obtained by slow diffusion of hexanes (~10 mL) into a solution of **2** (~40 mg) in $C_2H_4Cl_2$ (~3 mL) at – 30 °C. ^{1}H NMR (CD_2Cl_2, 600 MHz, 298 K): δ 7.97 (d, $^3J_{H,H}$ 8 Hz, 1H, C*H*^{6}), 7.96–7.92 (m, 2H, *o*-P*Ph*$_2$ A), 7.81 (d, $^3J_{H,H}$ 7 Hz, 2H, *o*-B*Ph*$_2$ A), 7.55–7.47 (m, 4H, C*H*^{5}, *m*,*p*-P*Ph*$_2$ A), 7.24–7.18 (m, 7H, C*H*^{4}, *m*,*p*-P*Ph*$_2$ B, *m*,*p*-B*Ph*$_2$ A), 7.08 (t, $^3J_{H,H}$ 7 Hz, 1H, C*H*^{3}), 6.80–6.76 (m, 2H, *o*-P*Ph*$_2$ B), 6.73 (t, $^3J_{H,H}$ 7 Hz, 2H, *m*-B*Ph*$_2$ B), 6.64–6.62 (m, 2H, *o*-B*Ph*$_2$ B), 6.45 (td, $^3J_{H,H}$ 7 Hz, $^4J_{H,H}$ 4 Hz, 1H, *p*-B*Ph*$_2$ B), 4.43 (d, $^3J_{H,H}$ 1 Hz, 1H, C*H*$^{2'/5'}$), 4.25 (q, $^3J_{H,H}$ 2 Hz, 1H, C*H*$^{3''/4''}$), 4.22–4.21 (m, 2H, C*H*$^{4'/3'}$, C*H*$^{4''/3''}$), 4.17 (q, $^3J_{H,H}$ 3 Hz, 1H, C*H*$^{3'/4'}$, C*H*$^{5'/2'}$), 4.12 (s, C*H*$^{2''/5''}$), 3.65 (app. septet, $^3J_{H,H}$ 1 Hz, 1H, C*H*$^{5''/2''}$), 0.98 (d, $^3J_{H,P}$ 14 Hz, 9H, C*Me*$_3$). ^{13}C{^{1}H} NMR (CD_2Cl_2, 151 MHz, 298 K): δ 161.3 (broad s, *C*^{2}), 152.0 (broad s, *ipso*-B*Ph*$_2$ A), 145.1 (dd, $^1J_{C,P}$ 36, $^3J_{C,P}$ 12 Hz, *C*$^{1'}$), 136.8 (d, $^1J_{C,P}$ 26 Hz, *ipso*-P*Ph*$_2$ A), 136.3 (d, $^1J_{C,P}$ 23 Hz, *ipso*-P*Ph*$_2$ B), 136.1 (d, $^2J_{C,P}$ 19 Hz, *o*-P*Ph*$_2$ A), 133.2 (app. d, *J* 6 Hz, *o*-B*Ph*$_2$ A), 133.0 (s, *p*-B*Ph*$_2$ A), 132.8 (dd, $^2J_{C,P}$ 33, $^4J_{C,P}$ 3 Hz, *C*^{6}), 132.3 (d, $^2J_{C,P}$ 14 Hz, *o*-P*Ph*$_2$ B), 130.6 (s, *p*-P*Ph*$_2$ A), 129.5 (s, *C*^{5}), 128.9 (app. d, *J* 4 Hz, *m*-B*Ph*$_2$ B), 128.7 (d, $^3J_{C,P}$ 10 Hz, *m*-P*Ph*$_2$ A), 128.4 (s, *p*-P*Ph*$_2$ B), 127.9 (d, $^3J_{C,P}$ 8 Hz, *m*-P*Ph*$_2$ B), 127.0 (app. d, *J* 5 Hz, *p*-B*Ph*$_2$ B), 126.9 (s, *m*-B*Ph*$_2$ A), 125.3 (d, $^4J_{C,P}$ 5 Hz, *C*^{4}), 125.1 (s, *C*^{3}), 121.3 (app. d, *J* 5 Hz, *o*-B*Ph*$_2$ B), 84.7 (dd, $^1J_{C,P}$ 27, $^3J_{C,P}$ 3 Hz, *C*$^{1'}$), 79.1 (d, $^1J_{C,P}$ 36 Hz, *C*$^{1''}$), 75.9 (d, $^2J_{C,P}$ 20 Hz, *C*$^{5'/2''}$), 75.7 (d, $^3J_{C,P}$ 9 Hz, *C*$^{5'/2'}$), 73.4 (d, $^3J_{C,P}$ 5 Hz, *C*$^{2''/5''}$), 72.0 (d, $^2J_{C,P}$ 7 Hz, *C*$^{2'/5'}$), 71.3 (d, $^2J_{C,P}$ 7 Hz, *C*$^{4''/3''}$), 71.0 (d, $^3J_{C,P}$ 3 Hz, *C*$^{3''/4''}$), 70.3 (d, $^3J_{C,P}$ 4 Hz, *C*$^{3'/4'}$), 70.0 (d, $^2J_{C,P}$ 5 Hz, *C*$^{4'/3'}$), 36.9 (d, $^1J_{C,P}$ 12 Hz, *C*Me$_3$), 29.5 (d, $^2J_{C,P}$ 7 Hz, C*Me*$_3$); *ipso*-B*Ph*$_2$ B could not be located. ^{31}P{^{1}H} (CD_2Cl_2, 203 MHz, 298 K): δ 43.9 (d, $^2J_{P,P}$ 19 Hz, C_5H_4P(*t*Bu)Ar), 11.9 (d, $^2J_{P,P}$ 19 Hz, C_5H_4PPh$_2$). ^{11}B NMR (CD_2Cl_2, 161 MHz, 298 K): δ 23 (broad s, $\omega_{1/2}$ = 1100 Hz). Anal. Calcd. For $C_{44.5}H_{42}BClFeP_2Pd$: C, 63.08; H, 5.00%. Found: C, 62.80; H, 5.25%.

FcPPP: Toluene (50 mL) was condensed into a 100 mL Schlenk flask containing [Fe(η^5-$C_5H_4PPh_2$){η^5-C_5H_4P(*t*Bu)(C_6H_4Br-*o*)}] (529 mg, 0.863 mmol) through the use of a dry ice/acetone bath. The toluene solution was cooled to –45 °C and a solution of ^{t}BuLi (111 mg, 1.73 mmol) in toluene (5 mL) was added dropwise. The reaction mixture was then warmed to 0 °C and left to stir at that temperature for 3.5 hours, during which time a fine, white precipitate had precipitated out of solution turning the previously transparent, orange solution opaque. The reaction mixture was then cooled to –45 °C and a solution of Cl–PPh_2 (190 mg, 0.863 mmol) in toluene (5 mL) was added dropwise; the reaction mixture then left to stir overnight while warming to room temperature. After stirring overnight the opaque, tangerine coloured solution was evaporated to dryness *in vacuo* to yield an orange oil. Hexanes (15 mL) were added to the crude oil and the mixture was sonicated for 15 minutes to dissolve the crude product; the hexanes solution was brought into the dry box and stored at –30 °C for several days. The hexanes mother liquors were decanted, and the remaining sunset orange solid was dried *in vacuo*. Yield = 480 mg (77 %). ^{1}H NMR (C_6D_6, 600 MHz, 298 K): δ 7.63–7.60 (m, 1H, C*H*^{6}), 7.52–7.50 (m, 2H, *o*-PPh_2^{Ar} A), 7.48–7.43 (m, 6H, *o*-PPh_2^{Ar} B, *o*-PPh_2^{Cp}), 7.26–7.23 (m, 1H, C*H*^{3}), 7.10–7.02 (m, 13H, C*H*^{5}, *m*,*p*-PPh_2^{Ar}, *m*,*p*-PPh_2^{Cp}), 6.98 (t, $^3J_{H,H}$ 8 Hz, 1H, C*H*^{4}), 4.35 (app. septet, $^3J_{H,H}$ 1 Hz, 1H, C*H*$^{2'/5'}$), 4.26 (s, 1H, C*H*$^{3''/4''}$), 4.17 (app. quintet, $^3J_{H,H}$ 1 Hz, 1H, C*H*$^{3'/4'}$), 4.15–4.11 (m, 3H, C*H*$^{4'/3'}$, C*H*$^{2''/5''}$, C*H*$^{4''/3''}$), 4.04–4.03 (m, 1H, C*H*$^{5'/2'}$), 3.98 (s, 1H, C*H*$^{5''/2''}$), 1.07 (d, $^3J_{H,P}$ 12 Hz, 9H, C*Me*$_3$). ^{13}C NMR (C_6D_6, 151 MHz, 298 K): δ 147.4 (dd, $^1J_{C,P}$ 37 Hz, $^2J_{C,P}$ 12 Hz, *C*^{2}), 143.7 (dd, $^1J_{C,P}$ 29 Hz, $^2J_{C,P}$ 18 Hz, *C*^{1}), 140.2 (dd, $^1J_{C,P}$ 17 Hz, $^4J_{C,P}$ 12 Hz, *ipso*-P$Ph_2^{Ar/Cp}$), 139.0–138.7 (app. m, *ipso*-P$Ph_2^{Ar/Cp}$), 136.1 (s, *C*^{6}), 135.1 (d, $^2J_{C,P}$ 20 Hz, *o*-PPh_2^{Ar} B), 134.7 (d, $^2J_{C,P}$ 20 Hz, *o*-PPh_2^{Ar} A), 134.1 (d, $^2J_{C,P}$ 9 Hz, *o*-PPh_2^{Cp}), 134.0 (d, $^2J_{C,P}$ 8 Hz, *o*-PPh_2^{Cp}), 133.9 (s, *C*^{3}), 129.6 (s, *C*^{4}), 128.9 (d, $^3J_{C,P}$ 7 Hz, *m*-P$Ph_2^{Ar/Cp}$), 128.8 (d, $^3J_{C,P}$ 6 Hz, *m*-P$Ph_2^{Ar/Cp}$), 128.7 (d, $^3J_{C,P}$ 6 Hz, *m*-P$Ph_2^{Ar/Cp}$), 128.6 (d, $^3J_{C,P}$ 8 Hz, *m*-P$Ph_2^{Ar/Cp}$), 128.5, 128.4, 128.4, 128.4 (4×s, *p*-P$Ph_2^{Ar/Cp}$), 128.0 (s, *C*^{5}), 77.6 (dd, $^1J_{C,P}$ 23 Hz, $^4J_{C,P}$ 7 Hz, *C*$^{1'}$), 77.0 (d, $^1J_{C,P}$ 8 Hz, *C*$^{1''}$), 75.8 (d, $^2J_{C,P}$ 26 Hz, *C*$^{2'/5'}$), 74.5 (d, $^2J_{C,P}$ 15 Hz, *C*$^{2''/5''}$), 74.1 (d, $^2J_{C,P}$ 15 Hz, *C*$^{5''/2''}$), 73.8 (s, *C*$^{3''/4''}$), 73.5 (s, *C*$^{4''/3''}$), 73.0 (s, *C*$^{5'/2'}$), 72.1 (s, *C*$^{4'/3'}$), 71.8 (d, $^3J_{C,P}$ 5 Hz, *C*$^{3'/4'}$), 32.7 (d, $^1J_{C,P}$ 16 Hz, *C*Me$_3$), 28.7 (d, $^2J_{C,P}$ 14 Hz, C*Me*$_3$). ^{31}P{^{1}H} NMR (C_6D_6, 203 MHz, 298 K): δ –7.5 (d, $^2J_{P,P}$ 176 Hz, C_5H_4P(*t*Bu)Ar), –11.2 (d, $^2J_{P,P}$ 176 Hz, Ar*P*Ph$_2$), –16.5 (s, C_5H_4PPh$_2$). Anal. Calcd. For $C_{44}H_{41}FeP_3$: C, 73.54; H, 5.75%. Found: C, 73.89; H, 6.00%.

"Ni(FcPPP)" (3): Toluene (10 mL) was condensed into a 50 mL round bottom flask containing [Ni(cod)$_2$] (50.4 mg, 0.183 mmol) and FcPPP (132 mg, 0.183 mmol) through the use of a dry ice/acetone bath, and the reaction was left to stir for three hours at room temperature. The ruby red reaction solution was evaporated to dryness *in vacuo* to yield a dark red oily residue. Hexamethyldisiloxane (20 mL) were added to the crude oil and the slurry was sonicated for 15 minutes, resulting in precipitation of a red/orange solid. The O(SiMe$_3$)$_2$ solution was filtered and the collected red/orange solid was washed with O(SiMe$_3$)$_2$ (10 mL) then dried *in vacuo*. Yield = 124 mg (87 %). ^{31}P{^{1}H} NMR (Toluene-d$_8$, 298 K, 203 MHz): δ 59.8 (appt. t, $^2J_{P,P}$ 40 Hz), 55.1 (broad s, $\omega_{1/2}$ ~100 Hz), 53.0 (broad s, $\omega_{1/2}$ ~100 Hz), 40.3 (broad s, $\omega_{1/2}$ ~100 Hz), 21.9 (broad s, $\omega_{1/2}$ ~100 Hz), 21.3 (broad s, $\omega_{1/2}$ ~100 Hz), 19.0 (broad s, $\omega_{1/2}$ ~100 Hz), 17.7 (broad s, $\omega_{1/2}$ ~100 Hz). Anal. Calcd. For $C_{44}H_{41}FeNiP_3$: C, 67.99; H, 5.32%. Found: C, 67.97; H, 5.37%.

***rac*-[{Ni(FcPPP)}$_2$(μ-N_2)] (4):** "Ni(FcPPP)" (118 mg, 0.151 mmol) was dissolved in a mixture of benzene (3 mL) and hexanes (10 mL) in a 50 mL Schlenk tube. The resulting solution was subjected to three freeze/pump/thaw cycles before the introduction of 1 atm of N_2. The Schlenk tube was sealed and the solution was maintained under N_2 at room temperature for 7 days, resulting in crystallization of **4** as ruby red crystals. The mother liquors were decanted, and the remaining crystalline material was dried *in vacuo*. Yield = 76.7 mg (64 %). X-ray quality crystals were obtained by slow diffusion of hexanes (~10 mL) into a solution of **4** (~30 mg) in benzene (~3 mL) at room temperature. ^{1}H NMR (THF-d$_8$, 600 MHz, 298 K): δ 8.13 (broad s, 2H, C*H*^{6}), 8.05 (t, $^3J_{H,H}$ 7 Hz, 4H, *o*-PPh_2^{Ar} A), 7.69–7.64 (broad m, 6H, C*H*^{3}, *o*-PPh_2^{Cp} A), 7.48–7.36 (m, 10H, C*H*^{4}, C*H*^{5}, *m*,*p*-PPh_2^{Ar} A), 6.97 (t, $^3J_{H,H}$ 7 Hz, 2H, *p*-PPh_2^{Cp} A), 6.85 (broad s, 4H, *o*-PPh_2^{Cp} B), 6.70 (t, $^3J_{H,H}$ 7 Hz, 2H, *p*-PPh_2^{Ar} B), 6.67–6.61 (m, 6H, *p*-PPh_2^{Cp} B, *o*-PPh_2^{Ar} B), 6.46 (t, $^3J_{H,H}$ 7 Hz, 4H, *m*-PPh_2^{Ar} B), 6.42 (t, $^3J_{H,H}$ 6 Hz, 4H, *m*-PPh_2^{Cp} A), 6.16 (broad s, 4H, *m*-PPh_2^{Cp} B), 4.77 (s, 2H, C*H*$^{2'/5'}$), 4.37 (s, 2H, C*H*$^{5'/2'}$), 4.12 (s, 2H, C*H*$^{3'/4'}$), 4.11 (s, 2H, C*H*$^{4'/3'}$), 3.95 (s, 2H, C*H*$^{3''/4''}$), 3.89 (s, 2H, C*H*$^{4''/3''}$), 3.38 (s, 2H, C*H*$^{2''/5''}$), 3.22 (s, 2H, C*H*$^{5''/2''}$), 1.50 (d, $^3J_{H,P}$ 13 Hz, 18H, C*Me*$_3$). ^{13}C NMR (THF-d$_8$, 151 MHz, 298 K): δ 149.2 (dd, $^1J_{C,P}$ 49 Hz, $^2J_{C,P}$ 35 Hz, *C*$^{1/2}$), 145.0 (dd, $^1J_{C,P}$ 45 Hz, $^2J_{C,P}$ 29 Hz, *C*$^{1/2}$), 144.2–144.0 (m, *ipso*-PPh_2^{Ar} A), 141.8–141.5 (m, *ipso*-PPh_2^{Cp} A/B), 139.7–139.4 (m, *ipso*-PPh_2^{Cp} A/B), 138.0–137.7 (m, *ipso*-PPh_2^{Ar} B), 136.3 (d, $^2J_{C,P}$ 15 Hz, *o*-PPh_2^{Cp} A), 134.6 (d, $^2J_{C,P}$ 13 Hz, *C*^{3}), 134.4 (d, $^2J_{C,P}$ 16 Hz, *o*-PPh_2^{Ar} A), 133.3 (d, $^2J_{C,P}$ 11 Hz, *C*^{6}), 131.8 (d, $^2J_{C,P}$ 12 Hz, *o*-PPh_2^{Ar} B), 129.4 (s, *C*^{4}), 129.1 (s, *C*^{5}), 128.5 (d, $^3J_{C,P}$ 8 Hz, *m*-PPh_2^{Ar} A, *p*-PPh_2^{Cp} A), 128.3 (d, $^3J_{C,P}$ 8 Hz, *m*-PPh_2^{Cp} A), 127.9 (broad s, *o*/*m*-PPh_2^{Cp} B), 127.8 (s, *p*-PPh_2^{Ar} A), 127.6 (broad s, *o*/*m*-PPh_2^{Cp} B), 127.1 (d, $^3J_{C,P}$ 6 Hz, *m*-PPh_2^{Ar} B), 126.7 (s, *p*-PPh_2^{Cp} B), 126.2 (s, *p*-PPh_2^{Ar} B), 84.7 (dd, $^1J_{C,P}$ 35 Hz, $^3J_{C,P}$ 4 Hz, *C*$^{1''}$), 83.4 (m, *C*$^{1'}$), 75.9 (d, $^2J_{C,P}$ 24 Hz, *C*$^{2'/5'}$), 74.7 (d, $^2J_{C,P}$ 23 Hz, *C*$^{2''/5''}$), 73.3 (s, *C*$^{5''/2''}$), 72.8 (s, *C*$^{5'/2'}$), 72.4, 72.3 (2×s, *C*$^{3'/4'}$, *C*$^{3''/4''}$), 69.0 (s, *C*$^{4'/3'}$, *C*$^{4''/3''}$), 35.7 (s, *C*Me$_3$), 29.7 (d, $^2J_{C,P}$ 10 Hz, C*Me*$_3$). ^{31}P{^{1}H} NMR (THF-d$_8$, 203 MHz, 298 K): δ 51.6 (broad d, $^2J_{P,P}$ ~ 84 Hz, C_5H_4P(*t*BuAr), 35.6 (broad dd, $^2J_{P,P}$ ~ 87 Hz, $^2J_{P,P}$ ~ 64 Hz, Ar*P*Ph$_2$), 19.2 (broad d, $^2J_{P,P}$ ~ 59 Hz, C_5H_4PPh$_2$).

Raman: ν(N≡N) = 2006 cm^{-1}. Anal. Calcd. For $C_{88}H_{82}Fe_2N_2Ni_2P_6$: C, 66.78; H, 5.22; N, 1.78%. Found: C, 66.44; H, 5.07; N, 1.72%.

[Pd(η²-dba)(FcPPP)] (5): Toluene (25 mL) was condensed into a 50 mL round bottom flask containing [$Pd_2(dba)_3$] (235 mg, 0.257 mmol) and FcPPP (369 mg, 0.513 mmol) through the use of a dry ice/acetone bath, and the reaction was left to stir overnight at room temperature. The black/yellow reaction solution was filtered to remove any unreacted [$Pd_2(dba)_3$], the residue was washed with 2 × 10 mL of toluene, and the resulting clear, blood orange filtrate was evaporated to dryness *in vacuo* to afford a red/orange, oily residue. Hexanes (30 mL) were added to the crude oil and the resulting mixture was sonicated for 15 minutes, allowing for [Pd(η²-dba)(FcPPP)] to precipitate from solution as a bright orange powder. The hexanes solution was filtered and the collected product was washed with hexanes (3 × 10 mL) then dried *in vacuo*. Yield = 412 mg (76 %). X-ray quality crystals were obtained by slow diffusion of hexanes (~10 mL) into a solution of **5** (~30 mg) in CH_2Cl_2 (~3 mL) at –30 °C. $^{31}P\{^1H\}$ NMR (C_6D_6, 298 K, 203 MHz): δ 60.2 (broad s, $\omega_{1/2}$ ~190 Hz), 57.3 (broad s, $\omega_{1/2}$ ~190 Hz), 55.7 (broad s, $\omega_{1/2}$ ~190 Hz), 38.9 (broad s, $\omega_{1/2}$ ~190 Hz), –16.7 (broad s, $\omega_{1/2}$ ~110 Hz). ^1H NMR (Toluene-d_8, 230 K, 500 MHz; selected data): δ 1.06 (d, $^3J_{H,P}$ 12 Hz, C*Me*$_3$), 0.99 (d, $^3J_{H,P}$ 14 Hz, C*Me*$_3$), 0.69 (d, $^3J_{H,P}$ 15 Hz, C*Me*$_3$), 0.40 (d, $^3J_{H,P}$ 15 Hz, C*Me*$_3$). Anal. Calcd. For $C_{61}H_{55}FeOP_3Pd$: C, 69.17; H, 5.23%. Found: C, 69.07; H, 5.45%.

In situ generation of [Ni(η²-dba)(FcPPP)] (6): Method A: "Ni(FcPPP)" (**3**) (12 mg, 1.5×10^{-2} mmol) and dba (3.6 mg, 1.5×10^{-2} mmol) were dissolved in C_6D_6 (0.6 mL) in an NMR tube at room temperature, causing the previously orange/red solution to become cherry red. The NMR scale reaction was maintained at room temperature for 2 hours. **Method B:** [{Ni(FcPPP)}$_2$(μ-N_2)] (**4**) (7.9 mg, 5.0×10^{-3} mmol) and dba (2.3 mg, 9.8×10^{-3} mmol) were dissolved in C_6D_6 (0.6 mL) in an NMR tube at room temperature. The NMR scale reaction was maintained at room temperature for 1 hour. Key NMR data: ^1H NMR (C_6D_6, 298 K, 500 MHz): δ 7.82 (s), 7.71 (s), 7.59 (s), 7.48 (broad s), 7.37 (broad s), 7.27–7.24 (m), 7.05 (s), 7.02 (s), 6.94–6.88 (m), 6.69 (broad s), 5.30 (s), 4.91 (s), 4.79 (s), 4.30 (s), 4.26 (s), 4.20 (s), 4.13 (s), 3.97 (s), 3.59 (s), 3.55 (s), 3.37 (s), 0.95 (d, $^3J_{H,P}$ 14 Hz, C*Me*$_3$), 0.71 (d, $^3J_{H,P}$ 14 Hz, C*Me*$_3$). $^{31}P\{^1H\}$ NMR (C_6D_6, 298 K, 203 MHz): δ 65.4 (d, $^2J_{P,P}$ 54 Hz, $C_5H_4P^tBuAr$), 50.2 (d, $^2J_{P,P}$ 54 Hz, Ar*P*Ph$_2$), –16.7, –16.9 (2×s, $C_5H_4PPh_2$).

ASSOCIATED CONTENT

Supporting Information

NMR spectra for complexes **1**–**6** and X-ray structure refinement details for **1**, **2**, **4** and **5**. This material and CIFs for these X-ray crystal structures are available free of charge via the Internet at http://pubs.acs.org.

AUTHOR INFORMATION

Corresponding Author

* Phone: (905) 525-9140, Fax: (905) 522-2509. E-mail: emslied@mcmaster.ca. The authors declare no competing financial interests.

ACKNOWLEDGMENT

D.J.H.E. thanks NSERC of Canada for a Discovery Grant and B.E.C. thanks the Government of Canada for an NSERC PGS-D scholarship. We are grateful to Hilary A. Jenkins for assistance with the structure refinement of complex **5**.

REFERENCES

(1) (a) Kameo, H.; Nakazawa, H. *Chemistry-an Asian Journal* **2013**, *8*, 1720-1734. (b) Amgoune, A.; Bouhadir, G.; Bourissou, D. *Top. Curr. Chem.* **2013**, *334*, 281-312. (c) Emslie, D. J. H.; Cowie, B. E.; Kolpin, K. B. *Dalton Trans.* **2012**, *41*, 1101-1117. (d) Amgoune, A.; Bourissou, D. *Chem. Commun.* **2011**, 859-871. (e) Bouhadir, G.; Amgoune, A.; Bourissou, D. *Adv. Organomet. Chem.* **2010**, *58*, 1-107. (f) Kuzu, I.; Krummenacher, I.; Meyer, J.; Armbruster, F.; Breher, F. *Dalton Trans.* **2008**, 5836-5865. (g) Fontaine, F.-G.; Boudreau, J.; Thibault, M. H. *Eur. J. Inorg. Chem.* **2008**, 5439-5454.

(2) (a) Hill, A. F.; Owen, G. R.; White, A. J. P.; Williams, D. J. *Angew. Chem. Int. Ed.* **1999**, *38*, 2759-2761. (b) Crossley, I. R.; Hill, A. F.; Willis, A. C. *Organometallics* **2005**, *24*, 1062-1064.

(3) (a) Blagg, R. J.; Charmant, J. P. H.; Connelly, N. G.; Haddow, M. F.; Orpen, A. G. *Chem. Commun.* **2006**, 2350-2352. (b) Tsoureas, N.; Haddow, M. F.; Hamilton, A.; Owen, G. R. *Chem. Commun.* **2009**, 2538-2540. (c) Owen, G. R.; Gould, P. H.; Charmant, J. P. H.; Hamilton, A.; Saithong, S. *Dalton Trans.* **2010**, *39*, 392-400. (d) Dyson, G.; Zech, A.; Rawe, B. W.; Haddow, M. F.; Hamilton, A.; Owen, G. R. *Organometallics* **2011**, *30*, 5844-5850. (e) Nuss, G.; Saischek, G.; Harum, B. N.; Volpe, M.; Gatterer, K.; Belaj, F.; Mösch-Zanetti, N. C. *Inorg. Chem.* **2011**, *50*, 1991-2001.

(4) Ambiphilic ligands have also been prepared in situ by hydroboration of a coordinated vinylphosphine or isonitrile ligand: (a) ref. 28d. (b) ref. 30. (c) ref. 39a.

(5) (a) Bontemps, S.; Gornitzka, H.; Bouhadir, G.; Miqueu, K.; Bourissou, D. *Angew. Chem. Int. Ed.* **2006**, *45*, 1611-1614. (b) Bontemps, S.; Bouhadir, G.; Gu, W.; Mercy, M.; Chen, C.-H.; Foxman, B. M.; Maron, L.; Ozerov, O. V.; Bourissou, D. *Angew. Chem. Int. Ed.* **2008**, *47*, 1481-1484.

(6) Bontemps, S.; Bouhadir, G.; Miqueu, K.; Bourissou, D. *J. Am. Chem. Soc.* **2006**, *128*, 12056-12057.

(7) Oakley, S. R.; Parker, K. D.; Emslie, D. J. H.; Vargas-Baca, I.; Robertson, C. M.; Harrington, L. E.; Britten, J. F. *Organometallics* **2006**, *25*, 5835-5838.

(8) Emslie, D. J. H.; Blackwell, J. M.; Britten, J. F.; Harrington, L. E. *Organometallics* **2006**, *25*, 2412-2414.

(9) Cowie, B. E.; Emslie, D. J. H. *Chem. Eur. J.* **2014**, *20*, 16899-16912.

(10) Tutusaus, O.; Ni, C. B.; Szymczak, N. K. *J. Am. Chem. Soc.* **2013**, *135*, 3403-3406.

(11) Dunne, J. F.; Manna, K.; Wiench, J. W.; Ellern, A.; Pruski, M.; Sadow, A. D. *Dalton Trans.* **2010**, *39*, 641-653.

(12) Zhao, X.; Otten, E.; Song, D. T.; Stephan, D. W. *Chem. Eur. J.* **2010**, *16*, 2040-2044.

(13) (a) Fischbach, A.; Bazinet, P. R.; Waterman, R.; Tilley, T. D. *Organometallics* **2008**, *27*, 1135-1139. (b) Fromel, S.; Kehr, G.; Frohlich, R.; Daniliuc, C. G.; Erker, G. *Dalton Trans.* **2013**, *42*, 14531-14536.

(14) Son, J.-H.; Pudenz, M. A.; Hoefelmeyer, J. D. *Dalton Trans.* **2010**, *39*, 11081-11090.

(15) Jana, R.; Blacque, O.; Jiang, Y. F.; Berke, H. *Eur. J. Inorg. Chem.* **2013**, 3155-3166.

(16) Suess, D. L. M.; Peters, J. C. *J. Am. Chem. Soc.* **2013**, *135*, 12580-12583.

(17) Harman, W. H.; Lin, T. P.; Peters, J. C. *Angew. Chem. Int. Ed.* **2014**, *53*, 1081-1086.

(18) Suess, D. L. M.; Peters, J. C. *J. Am. Chem. Soc.* **2013**, *135*, 4938-4941.

(19) Harman, W. H.; Peters, J. C. *J. Am. Chem. Soc.* **2012**, *134*, 5080-5082.

(20) Cowie, B. E.; Emslie, D. J. H.; Jenkins, H. A.; Britten, J. F. *Inorg. Chem.* **2010**, *49*, 4060-4072.

(21) Sircoglou, M.; Bontemps, S.; Mercy, M.; Miqueu, K.; Ladeira, S.; Saffon, N.; Maron, L.; Bouhadir, G.; Bourissou, D. *Inorg. Chem.* **2010**, *49*, 3983-3990.

(22) Emslie, D. J. H.; Harrington, L. E.; Jenkins, H. A.; Robertson, C. M.; Britten, J. F. *Organometallics* **2008**, *27*, 5317-5325.

(23) Moret, M. E.; Peters, J. C. *J. Am. Chem. Soc.* **2011**, *133*, 18118-18121.

(24) Fong, H.; Moret, M. E.; Lee, Y.; Peters, J. C. *Organometallics* **2013**, *32*, 3053-3062.

(25) Malacea, R.; Chahdoura, F.; Devillard, M.; Saffon, N.; Gomez, M.; Bourissou, D. *Adv. Synth. Catal.* **2013**, *355*, 2274-2284.

(26) Moret, M. E.; Peters, J. C. *Angew. Chem. Int. Ed.* **2011**, *50*, 2063-2067.

(27) (a) Vergnaud, J.; Ayed, T.; Hussein, K.; Vendier, L.; Grellier, M.; Bouhadir, G.; Barthelat, J.-C.; Sabo-Etienne, S.; Bourissou, D. *Dalton Trans.* **2007**, 2370-2372. (b) Bontemps, S.; Bouhadir, G.; Apperley, D. C.; Dyer, P. W.; Miqueu, K.; Bourissou, D. *Chem. Asian. J.* **2009**, *4*, 428-435. (c) D. J. H. Emslie; B. E. Cowie; S. R. Oakley; N. L. Huk; H. A. Jenkins; L. E. Harrington; Britten, J. F. *Dalton Trans.* **2012**, *41*, 3523-3535.

(28) (a) Owen, G. R. *Chem. Soc. Rev.* **2012**, *41*, 3535-3546, and references therein. (b) Lin, T. P.; Peters, J. C. *J. Am. Chem. Soc.* **2013**, *135*, 15310-15313. (c) Anderson, J. S.; Rittle, J.; Peters, J. C. *Nature* **2013**, *501*, 84-88. (d) Ostapowicz, T. G.; Merkens, C.; Holscher, M.; Klankermayer, J.; Leitner, W. *J. Am. Chem. Soc.* **2013**, *135*, 2104-2107. (e) MacMillan, S. N.; Harman, W. H.; Peters, J. C. *Chem. Sci.* **2014**, *5*, 590-597.

(29) Anderson, J. S.; Moret, M. E.; Peters, J. C. *J. Am. Chem. Soc.* **2013**, *135*, 534-537.

(30) Barnett, B. R.; Moore, C. E.; Rheingold, A. L.; Figueroa, J. S. *J. Am. Chem. Soc.* **2014**, *136*, 10262-10265.

(31) Kameo, H.; Nakazawa, H. *Organometallics* **2012**, *31*, 7476-7484.

(32) Cowie, B. E.; Emslie, D. J. H. *Organometallics* **2013**, *32*, 7297-7305.

(33) (a) Crossley, I. R.; Hill, A. F. *Dalton Trans.* **2008**, 201-203. (b) Tsoureas, N.; Kuo, Y.-Y.; Haddow, M. F.; Owen, G. R. *Chem. Commun.* **2011**, *47*, 484-486.

(34) Zhu, J.; Mukherjee, D.; Sadow, A. D. *Chem. Commun.* **2012**, *48*, 464-466.

(35) Cowie, B. E.; Emslie, D. J. H. *Organometallics* **2015**, *34*, 2737–2746.

(36) (a) Turculet, L.; Feldman, J. D.; Tilley, T. D. *Organometallics* **2004**, *23*, 2488-2502. (b) Khaskin, E.; Zavalij, P. Y.; Vedernikov, A. N. *Angew. Chem. Int. Ed.* **2007**, *46*, 6309-6312. (c) Khaskin, E.; Zavalij, P. Y.; Vedernikov, A. N. *J. Am. Chem. Soc.* **2008**, *130*, 10088-10089. (d) Pal, S.; Vedernikov, A. N. *Dalton Trans.* **2012**, *41*, 8116-8122. (e) Pal, S.; Zavalij, P. Y.; Vedernikov, A. N. *Chem. Commun.* **2014**, *50*, 5376-5378.

(37) (a) Figueroa, J. S.; Melnick, J. G.; Parkin, G. *Inorg. Chem.* **2006**, *45*, 7056-7058. (b) Pang, K.; Tanski, J. M.; Parkin, G. *Chem. Commun.* **2008**, 1008-1010.

(38) Crossley, I. R.; Hill, A. F.; Willis, A. C. *Organometallics* **2007**, *26*, 3891-3895.

(39) (a) Miller, A. J. M.; Labinger, J. A.; Bercaw, J. E. *J. Am. Chem. Soc.* **2008**, *130*, 11874-11875. (b) Miller, A. J. M.; Labinger, J. A.; Bercaw, J. E. *Organometallics* **2010**, *29*, 4499-4516. (c) Miller, A. J. M.; Labinger, J. A.; Bercaw, J. E. *Organometallics* **2011**, *30*, 4308-4314.

(40) Moret, M. E.; Zhang, L. M.; Peters, J. C. *J. Am. Chem. Soc.* **2013**, *135*, 3792-3795.

(41) Direct comparisons have been made between complexes of neutral $B\{C_6H_4(PR_2)\text{-}o\}_3$ and monoanionic $Si\{C_6H_4(PR_2)\text{-}o\}_3$ ligands with the same overall charge, but different electronic configurations. See for example: (a) Suess, D. L. M.; Tsay, C.; Peters, J. C. *J. Am. Chem. Soc.* **2012**, *134*, 14158-14164. (b) ref. 24.

(42) Ziebart, C.; Federsel, C.; Anbarasan, P.; Jackstell, R.; Baumann, W.; Spannenberg, A.; Beller, M. *J. Am. Chem. Soc.* **2012**, *134*, 20701-20704.

(43) Lee, Y.; Mankad, N. P.; Peters, J. C. *Nat. Chem.* **2010**, *2*, 558-565.

(44) Zank, J.; Schier, A.; Schmidbaur, H. *J. Chem. Soc. Dalton Trans.* **1999**, 415-420.

(45) Sircoglou, M.; Bontemps, S.; Mercy, M.; Saffon, N.; Takahashi, M.; Bouhadir, G.; Maron, L.; Bourissou, D. *Angew. Chem. Int. Ed.* **2007**, *46*, 8583-8586.

(46) Lee, Y.; Peters, J. C. *J. Am. Chem. Soc.* **2011**, *133*, 4438-4446.

(47) Kim, Y. E.; Kim, J.; Lee, Y. *Chem. Commun.* **2014**, *50*, 11458-11461.

(48) Brown, H. C.; Racherla, U. S. *J. Org. Chem.* **1986**, *51*, 427-432.

(49) Kolpin, K. B.; Emslie, D. J. H. *Angew. Chem. Int. Ed.* **2010**, *49*, 2716-2719.

(50) Cook, K. S.; Piers, W. E.; Woo, T. K.; McDonald, R. *Organometallics* **2001**, *20*, 3927-3937.

(51) Cook, K. S.; Piers, W. E.; Rettig, S. J. *Organometallics* **1999**, *18*, 1575-1577.

(52) Holland, P. L. *Dalton Trans.* **2010**, *39*, 5415-5425.

(53) Kim, Y.-E.; Oh, S.; Kim, S.; Kim, O.; Kim, J.; Han, S. W.; Lee, Y. *J. Am. Chem. Soc.* **2015**, *137*, 4280-4283.

(54) Majchrzak, M.; Kostera, S.; Kubicki, M.; Kownacki, I. *Dalton Trans.* **2013**, *42*, 15535-15539.

(55) Comanescu, C. C.; Iluc, V. M. *Inorg. Chem.* **2014**, *53*, 8517-8528.

(56) Burger, B. J.; Bercaw J. E. *Vacuum Line Techniques for Handling Air-Sensitive Organometallic Compounds*. In *Experimental Organometallic Chemistry: A Practicum in Synthesis and Characterization*; Wayda, A. L., Darensbourg, M. Y., Eds.; ACS Symp. Ser.; American Chemical Society: Washington D.C., 1987, Vol. 357, pp 79-98.

(57) Sluis, P. V. D.; Spek, A. L. *Acta Crystallogr.* **1990**, *A46*, 194-201.